

Numerical Analysis of Explosion Characteristics of Vent Gas from 18650 LiFePO₄ Batteries with Different SOC_s

Shi-Lin Wang ^a, Xu Gong ^a, Li-Na Liu ^a, Yi-Tong Li ^a, Chen-Yu Zhang ^a, Le-Jun Xu ^a, Xu-Ning Feng ^b, Huai-Bin Wang ^{a,*}

^a China People's Police University

Langfang 065000, China

E-mail: wanghuaibin@cpperu.edu.cn

^b State Key Laboratory of Automotive Safety and Energy

Tsinghua University

Beijing 100084, China

Keywords: Combustion and explosion characteristics • explosion limit • laminar flame speed • adiabatic flame temperature • sensitivity analysis

Abstract: The combustion and explosion characteristics of lithium-ion battery vent gas is a key factor in determining the fire hazard of lithium-ion batteries. Therefore, investigating the combustion and explosion hazards of lithium-ion batteries vent gas can provide guidance for rescue and protection in explosion accidents in energy storage stations and new energy vehicles, thereby promoting the application and development of lithium-ion batteries. Based on this understanding and combined with previous research on gas production from lithium-ion batteries, this article conducted a study on the combustion and explosion risk of vent gas from thermal runaway of 18650 LFP batteries with different SOC_s. The explosion limit of mixed gases affected by carbon dioxide inert gas is calculated through the "elimination" method, and the Chemkin-Pro software is used to numerically simulate the laminar flame speed and adiabatic flame temperature of the battery vent gas. And the concentration of free radicals and sensitivity coefficients of major elementary reactions in the system are analyzed to comprehensively evaluate the combustion explosion hazard of battery vent gas. The study found that the 100% SOC battery has the lowest explosion limit of the vent gas. The inhibitory elementary reaction sensitivity coefficient in the reaction system is lower and the concentration of free radicals is higher. Therefore, it has the maximum laminar flame speed and adiabatic flame temperature. The combustion and explosion hazard of battery vent gas increases with the increase of SOC, and the risk of explosion is greatest and most harmful when SOC reaches 100%. However, the related hazards decrease to varying degrees with overcharging of the battery. This article provides a feasible method for analyzing the combustion mechanism of vent gas from lithium-ion batteries, revealing the impact of SOC on the hazardousness of battery vent gas. It provides references for the safety of storage and transportation of lithium-ion batteries, safety protection of energy storage stations, and the selection of related fire extinguishing agents.

Nomenclature

Abbreviation

LIB	Lithium-ion Battery	TR	Thermal Runaway
EL	Explosion Limit	LEL	Lower Explosion Limit
UEL	Upper Explosion Limit	LFS	Laminar Flame Speed
AFT	Adiabatic Flame Temperature	PLFC	Premixed Laminar Flame-speed Calculation

Introduction

Fuel shortage and air pollution are among the major concerns of current and future energy issues. New energy vehicles, especially electric vehicles, have been developed to meet the challenges of fuel shortage and air pollution [1, 2]. Many countries are using new energy vehicles as a substitute for traditional fuel vehicles to reduce dependence on oil and pollution of the environment [3, 4]. Against this background, China's new energy vehicle industry has developed rapidly. As of 2022, China has a total of 14.1 million new energy vehicles, including 11 million electric vehicles, with a battery demand of 25,000 GWh [5]. The power batteries are the core component of electric vehicles, and LIBs (lithium-ion batteries) are widely used in the field of electric vehicles due to their superior performance [6, 7]. However, LIBs themselves are relatively active and are prone to trigger TR (thermal runaway) under conditions of thermal abuse, electrical abuse, mechanical abuse, and electrochemical abuse, causing serious thermal accidents [8-10]. According to data from the National Emergency Management Department, a total of 640 new energy vehicle fires occurred in the first quarter of 2022, an increase of 32% compared with the same period. New energy vehicle fire accidents caused by TR of LIBs pose a great threat to people's lives and property safety, and also limit the commercial application of LIBs and the development of new energy vehicle industry [11, 12].

1 TR of LIBs can release a large amount of flammable and toxic
 2 gas. It can be ignited by high-temperature solid emissions or
 3 friction, thus forming jet flames and stable combustion of
 4 emissions [13]. Koch [14] et al. analyzed the TR eruption products
 5 of 51 LIBs, which mainly consisted of gases such as CO₂, CO,
 6 H₂, CH₄, C₂H₄, C₂H₆ and C₃H₆. Zhang [15] et al. conducted a
 7 study on the explosion limit (EL) of TR gases in NCM batteries
 8 with different SOC, and found that as the SOC increases, the
 9 lower explosion limit (LEL) of the vent gas first increases and
 10 then decreases, while the upper explosion limit (UEL) continues
 11 to increase. Baird [16] et al. calculated the EL, laminar flame
 12 speed (LFS), and maximum overpressure of the vent gases from
 13 different cathode materials in LIBs using a model. They found
 14 that NCA and LCO batteries generate higher flame speeds and
 15 maximum overpressures compared to LFP batteries. LFP
 16 batteries also have a higher LEL, which may reduce the
 17 probability of a flammable ignition.

18 There are numerous studies on the combustion of low carbon
 19 alkane fuels, for example, Hu [17] et al. simulated the premixed
 20 laminar flow combustion and ignition process of C1-C4 alkane
 21 fuels and analyzed the chemical reaction kinetics using Chemkin
 22 software. A similar analytical approach allows the ignition and
 23 explosion characteristics of LIBs vent gas to be analyzed. Ma [18]
 24 et al. investigated the EL and influencing factors of TR vent gas
 25 from LIBs using Chemkin software. Fan [19] et al. further added
 26 the components of the electrolyte and explored the EL, LFS,
 27 flame temperature, and heat release.

28 This paper calculates the EL of battery vent gas based on the
 29 composition and content of 18650 LFP battery vent gas with
 30 different SOCs. The Chemkin-Pro software is used to explore
 31 the LFS and AFT (adiabatic flame temperature) of the mixed
 32 gases, and sensitivity analysis of LFS of elementary reactions is
 33 conducted under the EL. This work can analyze the gas
 34 explosion risk and hazards of 18650 LFP batteries with different
 35 SOCs, providing guidance for the storage and transportation
 36 safety of LFP batteries.

37 Results and Discussion

38 Vent Gas Composition and Content

39 The detailed component contents of the vent gas from LFP
 40 batteries with different SOC are shown in Table 1. This data
 41 comes from Reference [20]. In the literature, the author
 42 constructed a custom-designed experimental platform. The main
 43 component of the test rig is a heatable reactor with electric
 44 feedthroughs for the temperature measurement and the inner
 45 sample heating. The device was evacuated and purged with
 46 argon twice, and then 1.1Ah18650 LFP batteries with different
 47 SOC were triggered in the heating sleeve to cause thermal
 48 runaway. Finally, collect the gas after cooling and analyze it
 49 using a gas chromatograph.

50 **Table 1.** Composition and content of vent gas from LFP
 51 batteries with different SOCs.

52

SOC (%)	H ₂ (%)	CO ₂ (%)	CO (%)	CH ₄ (%)	C ₂ H ₄ (%)	C ₂ H ₆ (%)
---------	--------------------	---------------------	--------	---------------------	-----------------------------------	-----------------------------------

0	2.7	93.4	1.8	0.7	0.7	0.7
25	7.1	85.3	3.1	1.2	3.1	0.2
50	20.8	66.2	4.8	1.6	6.6	-
75	21.8	62.6	6.4	1.9	6.3	1
100	29.4	48.4	9.1	5.4	7.2	0.5
115	34	52.2	6.4	2.6	4.7	0.1
130	30.1	55.8	7.7	6.4	-	-

It can be seen that CO₂ has the highest content among the six main gas components, and its content decreases with the increase of SOC until it reaches the lowest level at 100% SOC. However, as the battery continues to be charged to the overcharged state, CO₂ content but gradually increased. H₂ is the main component that determines the explosion hazard of gas mixture. Its content continues to increase as SOC increases until it reaches a peak at 115% SOC, and then begins to decline.

Numerical Simulation Calculation Methods

In this paper, the LFS of the battery vent gas/air is calculated using the PLFC (Premixed Laminar Flame-speed Calculation) model of Chemkin-Pro. PLFC is one of the 22 models that comes with Chemkin-Pro. It can simplify three-dimensional flames into one-dimensional premixed models. It solves the governing system of differential equations describing flame dynamics using an implicit finite difference method combined with time dependency and steady-state assumptions. In addition, its solution algorithm adopts an automatic coarse-to-fine grid refinement method to enhance the convergence of the steady-state method and provide an optimal grid layout.

The conditions for numerical simulation are normal temperature and pressure (298K, 0.101MPa). In addition, the EQUIL module is used to calculate the AFT in the equilibrium state under the conditions of normal pressure and enthalpy. The composition of the reactants is determined by the volume fraction, and the proportions are determined by the equivalent ratio. In the software, both GARD and CURV are set to 0.05, and the number of grids is set between 400 and 500, which can meet the requirements of grid independence and reduce the flame speed error.

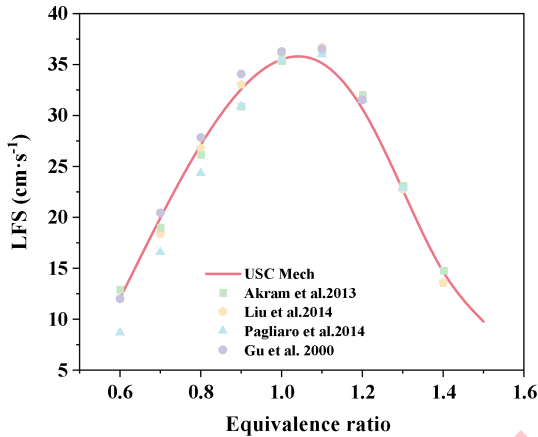
The USC Mech mechanism file used in this paper is the combustion kinetic mechanism for the H₂/CO/C1-C4 system constructed by Wang [21] et al. at USC, which has reactants that match the main components of the experimentally measured vent gases from LIBs.

Feasibility Verification

In order to verify the reliability of the PLFC model, the USC Mech mechanism was used to calculate the LFS of CH₄/air within a certain equivalence ratio range, and compared with the literature results under normal conditions [22-25], the results are shown in Fig.1.

Through comparison, it is found that in different CH₄/air LFS test experiments, there are some differences in the range of values

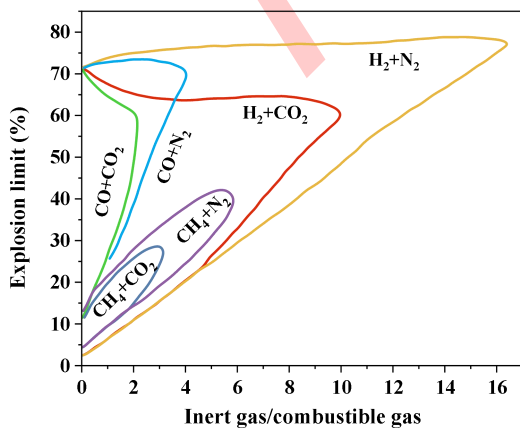
1 of equivalence ratios, and the LFS under the same equivalence
 2 ratios are also different, but in general have a similar trend of
 3 change. The maximum LFS all appeared between $\phi=1.0-1.1$,
 4 ranging from 35.8-36.7 cm/s. The simulation results are higher
 5 on the lean flame side than those of Pagliaro, with a difference
 6 of 3.3 cm/s at $\phi = 0.6$. However, the rest of the literature results
 7 are in good agreement with the USC Mech simulations, with an
 8 error range within 8%, which indicates that the Chemkin-Pro
 9 software can provide reasonable simulation results for LFS.
 10



11
12
13 **Figure 1.** Laminar flame speed of CH₄/air.

14 **Explosion Limits of Vent Gas**

15 The EL is one of the important parameters for evaluating the
 16 explosion characteristics of flammable gases. Studying the EL of
 17 vent gas from LIBs can determine the threshold for explosion
 18 hazards of LIBs during transportation, use and storage. This
 19 method is to "pair" a certain inert gas in the mixed gas with a
 20 certain combustible gas and consider it as a "new combustible
 21 gas", and find its corresponding EL based on the test curve in
 22 Fig.2 [26]. For example, if H₂ and CO₂ in the vent gas of a 100%
 23 SOC LFP battery are combined into a new gas, the volume
 24 percentage of the new gas H₂ + CO₂ is 77.8%, and the ratio of
 25 CO₂ to H₂ is 1.65. According to Fig.2, the UEL of H₂+CO₂ is
 26 65.9% and the LEL is 9.9%.
 27



28
29 **Figure 2.** Explosion limits of gas components.

Since the CO₂ content in the vent gas of 0% and 25% SOC LFP
 batteries far exceeds that of other combustible gas components,
 the volume fraction of any combustible gas after pairing is
 outside the EL, so the mixed gas cannot burn or explode, and
 there is no relevant explosion hazard analysis. Table 2 lists the
 ELs of H₂+CO₂ in batteries above 50% SOC, the values in the
 table are substituted into the Lechteilier formula to calculate the
 EL of the gas mixture.

Table 2. Explosion limits of gas components.

EL	H ₂ +CO ₂ (50%)	H ₂ +CO ₂ (75%)	H ₂ +CO ₂ (100%)	H ₂ +CO ₂ (115%)	H ₂ +CO ₂ (130%)
UEL	64.2%	64.1%	65.9%	66.3%	65.2%
LEL	16.7%	11.9%	9.9%	9.3%	10.9%

$$L = \frac{100}{\frac{V_1}{L_1} + \frac{V_2}{L_2} + \frac{V_3}{L_3} + \dots + \frac{V_n}{L_n}} \times 100\% \quad (1)$$

In the formula, L is the EL of LIB vent gas; L₁, L₂, and L₃ are the
 ELs of each component of the mixed gas; V₁, V₂, and V₃ are the
 concentration (volume fraction) of each component in the mixed
 gas. The ELs of vent gas from 18650 LFP batteries with different
 SOC are shown in Table 3.

Table 3. Explosion limits of battery vent gas.

EL	50% SOC	75% SOC	100% SOC	115% SOC	130% SOC
UEL	45.5%	61.7%	55.8%	61.4%	54.5%
LEL	12.4%	11.9%	8.2%	11.8%	10.2%

Fig.3 shows the EL range of vent gas from 18650 LFP batteries
 with different SOC. Under normal charging conditions, as the
 SOC increases, the LEL of the vent gas decreases, reaching the
 lowest point of 8.2% at 100% SOC. In the overcharged state, the
 LEL of the battery vent gas first rises and then decreases, but is
 still higher than the value of 100% SOC, which indicates that the
 100% SOC 18650 LFP battery vent gas is more susceptible to
 explosion hazards. As for the UEL, there is no obvious regularity.
 The UEL of 100% SOC is lower than that of 75% and 115%
 SOC. This is because the Lechteilier formula has a larger
 deviation when calculating the UEL, especially for mixed gases
 containing H₂, CH₄ and C₂H₄ [27].

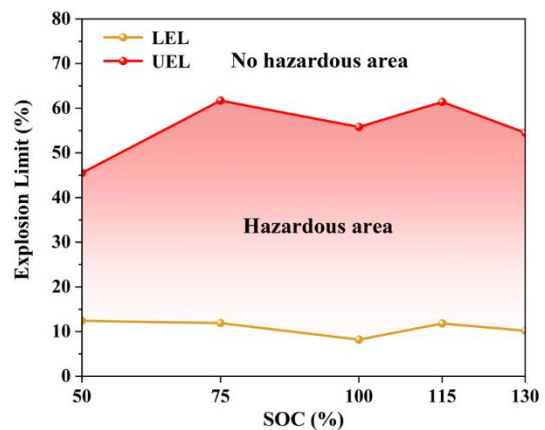


Figure 3. Explosion limits of vent gas from LFP batteries with different SOC.

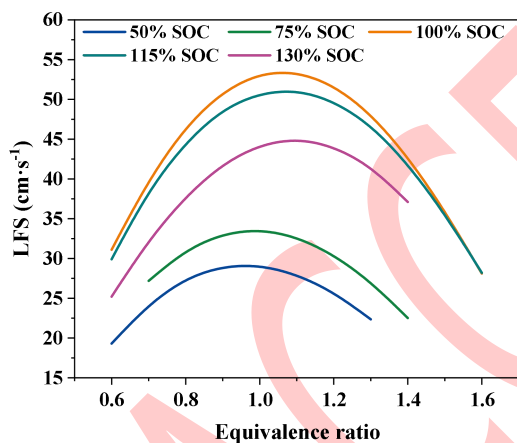
1

2 Laminar Flame Speed of the Vent Gas

3 The LFS is an inherent characteristic of combustible gas and is
4 a parameter that represents the danger of explosion when the
5 gas is ejected. It can quantify the danger of explosion of LIBs
6 vent gas in a confined space [28]. The vent gas from the battery
7 during TR may undergo combustion in a premixed mode, posing
8 a risk of explosion.

9 Fig.4 shows the LFS of the vent gas from 18650 LFP batteries at
10 different SOC calculated using Chemkin-Pro. Due to the varying
11 composition of the vent gas at different SOC, the range of LFS
12 of the vent gas/air also differs. However, the peak LFS occurs
13 between $\phi=1.0-1.1$ for all SOC. The peak LFS of the vent gas
14 from the batteries at different SOC, from low to high, are 29.2
15 cm/s, 33.7 cm/s, 53.5 cm/s, 51.2 cm/s, and 45.1 cm/s.

16 It can be seen that as the SOC increases, the LFS of the battery
17 vent gas increases overall. Until 100% SOC, the LFS value is
18 the highest under the full equivalence ratio. As the battery
19 continues to charge and enters the overcharged state, the LFS
20 begins to decrease with the increase of SOC. This is because
21 the CO_2 content in the vent gas from the 100% SOC 18650 LFP
22 battery is the lowest, resulting in the weakest inhibition effect on
23 the LFS.



24

25

26 **Figure 4.** Laminar flame speed of vent gas from LFP batteries
27 with different SOC.

28

29 Adiabatic Flame Temperature of the Vent Gas

30 The AFT is the temperature that the combustion products can
31 reach when the fuel achieves complete combustion under
32 adiabatic conditions. Although its value is higher than the actual
33 flame temperature, it can still be used as an important parameter
34 to evaluate the hazards of combustion heat of LIBs vent gas.

Fig. 5 shows the AFT of the vent gas from 18650 LFP batteries
with different SOC calculated by Chemkin-Pro. The trend of
AFT with SOC is similar to that of LFS, with the maximum value
occurring at $\phi = 1.0$. The AFT of the combustion of the battery
vent gas rises with the increase of SOC until the highest
temperature value at the full-equivalent ratio at 100% SOC. As
the battery continues to charge and enters overcharge state, the
temperature starts to decrease with increasing SOC. It is worth
noting that the AFT of the battery vent gas at 130% SOC is the
lowest. This is because the composition analysis of the battery
vent gases at 130% SOC does not include C_2H_4 and C_2H_6 ,
which are the main contributors to heat generation.

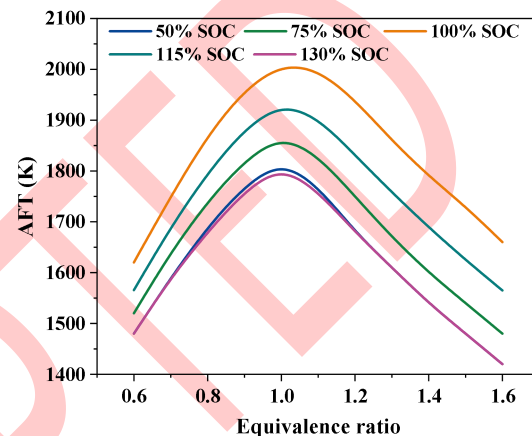


Figure 5. Adiabatic flame temperature of vent gas from LFP
batteries with different SOC.

Analysis of Free Radical Concentration

The mass fractions of H , O and OH radicals can reflect the
reaction rate of the system, especially the H radicals play an
important role in increasing the chemical reaction rate. Fig. 6
shows the variation of H , O and OH radical concentrations with
axial distance at the maximum LFS equivalent ratio in the vent
gas/air combustion system of 18650 LFP batteries with different
SOCs. In the same system, the OH radical concentration is the
highest, the H radical concentration is the lowest, and the O and
 OH radical concentrations are one order of magnitude higher
than the H radicals. The change pattern of H radical equilibrium
concentration in the reaction system of different SOC batteries
vent gas is consistent with the LFS, that is, 100% SOC > 115%
SOC > 130% SOC > 75% SOC > 50% SOC. The peak
concentration and equilibrium concentration of O and OH
radicals in the 100% SOC battery vent gas reaction system are
higher than those in other systems, which also shows that the
100% SOC battery vent gas combustion reaction rate is the
highest.

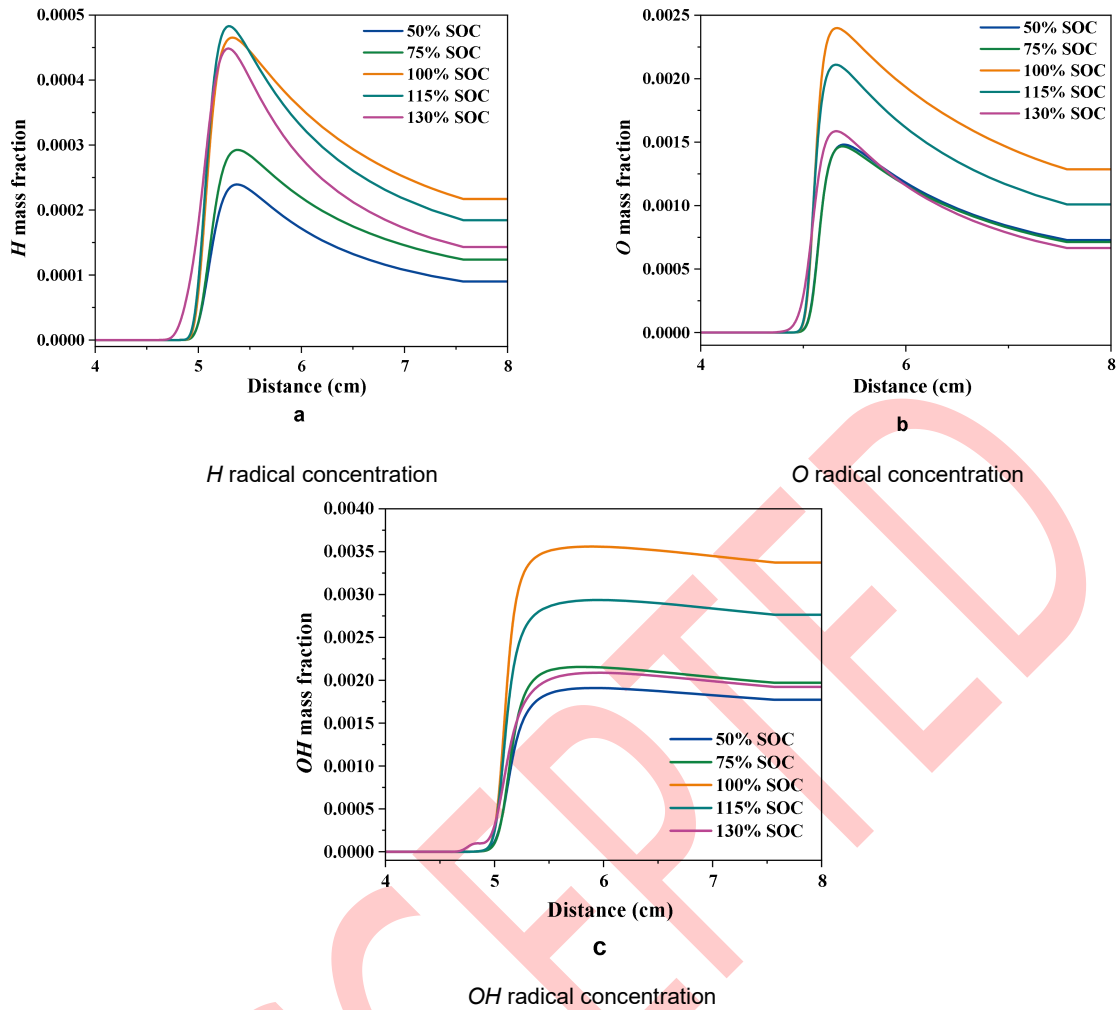


Figure 6. Free radical concentration in the reaction system of LFP batteries vent gas with different SOC.

Analysis of Free Radical Concentration

1 There are many elementary reactions involved in the
 2 combustion process of LIBs vent gas, but only a small part of
 3 them play a leading role in the entire combustion process.
 4 Therefore, in order to further analyze the most important
 5 reactions that affect the LFS, this paper carried out an
 6 elementary reaction sensitivity analysis of the LFS of different
 7 SOC batteries vent gas/air flames.
 8 Fig. 7 shows the five elementary reactions with the largest
 9 sensitivity coefficients under the maximum LFS equivalence
 10 ratio in different SOC batteries vent gas/air combustion reaction
 11 systems. A positive sensitivity coefficient indicates that the LFS
 12 increases with the increase in reaction rate constant, while a
 13 negative coefficient indicates a decrease. The sensitivity
 14 coefficient of R1 is much higher than that of other elementary
 15 reactions. This is because the chain branching reaction
 16 $H+O_2 \rightleftharpoons O+OH$, which starts with *H* atoms, plays a significant
 17 promoting role in the combustion process, and a series of large
 18 molecular groups need to react through the collision of free
 19 radicals.

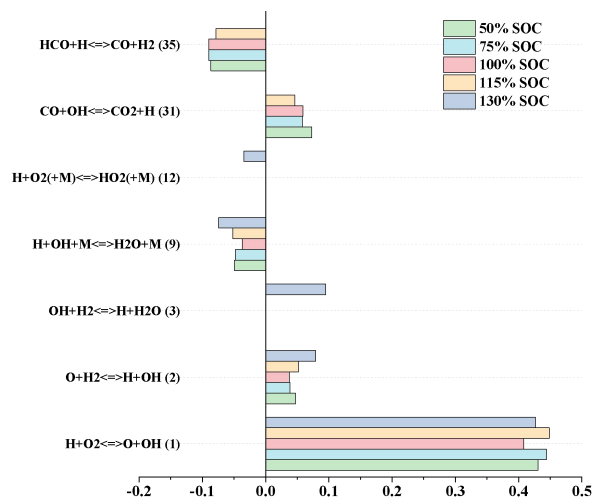


Figure 7. Sensitivity analysis of battery vent gas/air combustion reactions.

Among the four elementary reactions with the largest sensitivity coefficients except R1, there are two elementary reactions each that promote and inhibit the LFS. Although the elementary

1 reactions with positive sensitivity coefficients are not the highest
 2 in the 100% SOC battery vent gas reaction system, the inhibiting
 3 effect of elementary reaction R9 is the lowest, so the LFS of the
 4 100% SOC battery vent gas is the highest.

5

6 Conclusion

7 This paper analyzes the risk of combustion and explosion of
 8 vent gas from 18650 LFP batteries with different SOCs,
 9 calculates the EL of the gas mixture and analyzes the
 10 combustion characteristics of the gas mixture by Chemkin-Pro
 11 software, and obtains the main conclusions as follow:

12 (1) Calculated the EL of vent gas from LIBs containing the inert
 13 gas CO₂, and found that the LEL of vent gas from 100% SOC
 14 batteries is lower and is more likely to reach the EL, causing the
 15 risk of explosion. In addition, the high CO₂ content in vent gas
 16 from batteries at 0% and 25% SOC prevents the mixture gas
 17 from undergoing combustion or explosion, making it a safe SOC
 18 for battery storage and transportation.

19 (2) The LFS and AFT of the vent gas/air both show a trend of
 20 first increasing and then decreasing as the equivalence ratio
 21 increases, with the maximum value appearing between $\varphi=1.0$ -
 22 1.1. As the SOC increases, the LFS and AFT of vent gas from
 23 the batteries increase overall, reaching the highest values at
 24 100% SOC under all equivalence ratios. As the battery
 25 continues to charge and enters the overcharged state, the LFS
 26 and AFT of vent gas start to decrease with the increase of SOC.

27 (3) The characteristics of the mixed gas combustion reaction can
 28 be analyzed through LFS sensitivity and free radical
 29 concentration. The 100% SOC battery vent gas/air combustion
 30 system has the highest concentration of H, O and OH free
 31 radicals, and the inhibitory elementary reaction sensitivity
 32 coefficient is lower, so it has a greater LFS and AFT.

33 To sum up, the 100% SOC 18650 LFP battery has a lower LEL
 34 of vent gas and is more prone to explosion risks. Moreover, after
 35 TR occurs, the LFS and AFT of the vent gas are higher than
 36 those of other batteries, which shows that the TR of 100% SOC
 37 18650 LFP battery has higher explosion hazard. In addition, the
 38 CO₂ content in the vent gas of 18650 LFP batteries at 0% and
 39 25% SOC accounts for more than 85%. All components in the
 40 mixed gas are outside the EL range and will not cause
 41 combustion. This work can provide a reference for the storage
 42 and transportation safety of LIBs, and guide the fire rescue work
 43 in thermal disaster accidents of energy storage stations and
 44 electric vehicles, so as to reduce the threat of personal and
 45 property safety caused by the TR of LIBs.

46 Acknowledgements

47 This work was supported by the National Natural Science
 48 Foundation of China (52106284) and the Natural Science
 49 Foundation of Hebei Province (B2021507001). The first author
 50 would also like to acknowledge the support of Project to
 51 Promote Innovation in Doctoral Research at CPPU
 52 (BSKY202302).

References

- [1] Song L, Zheng Y, Xiao Z, Wang C, Long T. Review on Thermal Runaway of Lithium-Ion Batteries for Electric Vehicles[J]. *J Electron Mater*,2021, 51(1): 30-46.
- [2] Feng X, Lu L, Ouyang M, Li J, He X. A 3d Thermal Runaway Propagation Model for a Large Format Lithium Ion Battery Module[J]. *Energy*,2016, 115: 194-208.
- [3] Feng X, Ouyang M, Liu X, Lu L, Xia Y, He X. Thermal Runaway Mechanism of Lithium Ion Battery for Electric Vehicles: A Review[J]. *ESM*,2018, 10: 246-267.
- [4] Duan J, Tang X, Dai H, Yang Y, Wu W, Wei X, Huang Y. Building Safe Lithium-Ion Batteries for Electric Vehicles: A Review[J]. *EER*,2019, 3(1): 1-42.
- [5] International Energy Agency: Global EV Data Explorer [DB/OL]. <https://www.iea.org/data-and-statistics>
- [6] Zhang H, Wang L, He X. Trends in a Study on Thermal Runaway Mechanism of Lithium-Ion Battery with LiNi_xMn_yCo_{1-x-y}O₂ Cathode Materials[J]. *Battery Energy*,2021, 1(1).
- [7] Liu Y, Mao Y, Wang H, Pan Y, Liu B. Internal Short Circuit of Lithium Metal Batteries under Mechanical Abuse[J]. *Int Mech Sci*,2023, 245.
- [8] Golubkov AW, Planteu R, Krohn P, Rasch B, Brunnsteiner B, Thaler A, Hacker V. Thermal Runaway of Large Automotive Li-Ion Batteries[J]. *RSC Adv*,2018, 8(70): 40172-40186.
- [9] Liu B, Jia Y, Yuan C, Wang L, Gao X, Yin S, Xu J. Safety Issues and Mechanisms of Lithium-Ion Battery Cell Upon Mechanical Abuse Loading: A Review[J]. *ESM*,2020, 24: 85-112.
- [10] Szabo I, Sirca AA, Scurtu L, Kocsis L, Hanches IN, Mariaşiu F. Comparative Study of Li-Ion 21700 Cylindrical Cell under Mechanical Deformation[J]. *IOP Conference Series: Materials Science and Engineering*,2022, 1256(1).
- [11] SUN F, Rui X, Zeyu C. Research Status and Analysis for Battery Safety Accidents in Electric Vehicles[J]. *Journal of Mechanical Engineering*,2019, 55(24).
- [12] Li Y, Liu X, Wang L, Feng X, Ren D, Wu Y, Xu G, Lu L, Hou J, Zhang W, Wang Y, Xu W, Ren Y, Wang Z, Huang J, Meng X, Han X, Wang H, He X, Chen Z, Amine K, Ouyang M. Thermal Runaway Mechanism of Lithium-Ion Battery with LiNi_{0.8}Mn_{0.1}Co_{0.1}O₂ Cathode Materials[J]. *Nano Energy*,2021, 85.
- [13] Peng Y, Yang L, Ju X, Liao B, Ye K, Li L, Cao B, Ni Y. A Comprehensive Investigation on the Thermal and Toxic Hazards of Large Format Lithium-Ion Batteries with Lifepo(4) Cathode[J]. *J Hazard Mater*,2020, 381: 120916.
- [14] Koch S, Fill A, Birke KP. Comprehensive Gas Analysis on Large Scale Automotive Lithium-Ion Cells in Thermal Runaway[J]. *JPS*,2018, 398: 106-112.
- [15] Zhang Q, Niu J, Yang J, Liu T, Bao F, Wang Q. In-Situ Explosion Limit Analysis and Hazards Research of Vent Gas from Lithium-Ion Battery Thermal Runaway[J]. *J Energy Storage*,2022, 56.
- [16] Baird AR, Archibald EJ, Marr KC, Ezekoye OA. Explosion Hazards from Lithium-Ion Battery Vent Gas[J]. *JPS*,2020, 446.
- [17] HU E J, HUANG Z, JIANG, Kinetic Study on Laminar Burning Velocities and Ignition Delay Times of C1-C4 Alkanes [J]. *Journal Eng Thermophys-RUS*, 2013, 34(3): 558-562
- [18] Ma B, Liu J, Yu R. Study on the Flammability Limits of Lithium-Ion Battery Vent Gas under Different Initial Conditions[J]. *ACS Omega*,2020, 5(43): 28096-28107.

- 1 [19] Fan R, Wang Z, Lu Y, Lin C, Guo W. Numerical Analysis on the
2 Combustion Characteristic of Lithium-Ion Battery Vent Gases and the
3 Suppression Effect[J]. *Fuel*,2022, 330.
- 4 [20] Golubkov AW, Scheikl S, Planteu R, Voitic G, Wiltsche H, Stangl C,
5 Fauler G, Thaler A, Hacker V. Thermal Runaway of Commercial 18650
6 Li-Ion Batteries with Lfp and Nca Cathodes – Impact of State of Charge
7 and Overcharge[J]. *RSC Adv*,2015, 5(70): 57171-57186.
- 8 [21] Wang H, You A V, Joshi S G, et al. USC Mech Version II. High-
9 Temperature Combustion Reaction Model of H₂/CO/C₁-C₄
10 Compounds [DB/OL]. 2018-06-20,
11 http://ignis.usc.edu/USC_Mech_II.htm
- 12 [22] Akram M, Saxena P, Kumar S. Laminar Burning Velocity of Methane–
13 Air Mixtures at Elevated Temperatures[J]. *Energy Fuels*,2013, 27(6):
14 3460-3466.
- 15 [23] Liu Z, Kim NI. An Assembled Annular Stepwise Diverging Tube for the
16 Measurement of Laminar Burning Velocity and Quenching Distance[J].
17 *Combust Flame*,2014, 161(6): 1499-1506.
- 18 [24] Pagliaro JL, Linteris GT, Sunderland PB, Baker PT. Combustion
19 Inhibition and Enhancement of Premixed Methane–Air Flames by Halon
20 Replacements[J]. *Combust Flame*,2015, 162(1): 41-49.
- 21 [25] Shang R, Zhang Y, Zhu M, Zhang Z, Zhang D, Li G. Laminar Flame
22 Speed of Co₂ and N₂ Diluted H₂/Co/Air Flames[J]. *Int J of Hydrogen*
23 *Energy*,2016, 41(33): 15056-15067.
- 24 [26] GUO C, ZHANG Q. Determination on explosion limit of pyrolysis gas
25 released by lithium-ion battery and its risk analysis [J]. *Journal of Safety*
26 *Science and Technology* 2016, 12(9):46-49
- 27 [27] Chen Y. *Industrial fire and explosion accident prevention* [M]. Beijing:
28 Chemical Industry Press, 2010.
- 29 [28] Wang H, Xu H, Zhang Z, Wang Q, Jin C, Wu C, Xu C, Hao J, Sun L, Du
30 Z, Li Y, Sun J, Feng X. Fire and Explosion Characteristics of Vent Gas
31 from Lithium-Ion Batteries after Thermal Runaway: A Comparative
32 Study[J]. *eTransportation*,2022, 13.

不同 SOC 的 18650 LiFePO₄ 电池排放气体燃爆特性的数值分析

王世林^a, 龚旭^a, 刘丽娜^a, 李奕彤^a, 张宸语^a, 许乐俊^a, 冯旭宁^b, 王淮斌^{a*}

(a. 中国人民警察大学, 廊坊 065000)

(b. 清华大学汽车安全与能源国家重点实验室, 北京 100084)

摘要: 锂离子电池排放气体的燃爆特性是决定锂离子电池火灾危险性的关键因素, 因此探究锂离子电池排放气体的燃爆危害性可以为储能电站和新能源汽车燃爆事故救援与防护提供指导, 从而促进锂离子电池的应用与发展。建立在这一认识之上, 结合前人关于锂离子电池产气的研究, 本文开展了不同 SOC 的 18650 磷酸铁锂电池热失控排放气体的燃爆风险研究。通过“消元”的方法计算含有二氧化碳惰性气体影响的混合气体爆炸极限, 利用 Chemkin-Pro 软件对电池排放气体/空气的层流火焰速度与绝热火焰温度进行数值模拟, 并对体系内的自由基浓度与主要基元反应敏感系数进行分析, 综合评估电池排放气体燃爆危害性。研究发现 100% SOC 电池排放气体的爆炸下限最低, 反应体系中具有抑制作用的基元反应敏感系数较低且自由基浓度更高, 因此具有最大的层流火焰速度与绝热火焰温度。电池排放气体燃爆危害随 SOC 增加而增加, 直至 100% SOC 时燃爆风险最大且危害性最高, 然而随着电池过充电相关危害性却有不同程度下降。本文为锂离子电池排放气体燃烧机理分析提供了可行的方法, 揭示了 SOC 对电池排放气体燃爆危害性的影响, 对锂离子电池储存与运输安全、储能电站安全防护及相关灭火剂的选择提供了参考。

关键词: 关键词 1; 燃爆特性 2; 爆炸极限 3; 层流火焰速度 4; 绝热火焰温度 5; 敏感性分析